Interactions of carbon nanotubes in a nematic liquid crystal. I. Theory

Yves Galerne*

Institut de Physique et Chimie des Matériaux de Strasbourg, UMR 7504 (CNRS–Université de Strasbourg), 23 rue du Læss, 67034 Strasbourg, France

(Received 24 February 2015; published 11 April 2016)

Elongated and rodlike objects such as carbon nanotubes (CNTs) are studied when immersed in a nematic liquid crystal. Their interaction energy in a uniform nematic field depends on their orientation relative to the director $\boldsymbol{n}$, and its minimum determines if they stabilize parallel or perpendicular to $\boldsymbol{n}$. Using free energy calculations, we deduce the orientation at equilibrium that they choose in a uniform director field $\boldsymbol{n}$ or when they are in contact with a splay-bend disclination line. Naturally, the CNT orientations also depend on the anchoring conditions at their surface. Essentially, three types of anchorings are considered, planar, homeotropic, and Janus anchorings in the cases of weak and strong anchoring strengths. In the presence of a splay-bend disclination line, they are attracted toward it and ultimately, they get out of the colloidal dispersion to stick on it. Their orientation relative to the line is found to be parallel or perpendicular to it, again depending on the anchoring conditions. When a sufficient number of particles are deposited on a disclination line, we finally obtain a micro- or nanonecklace in the shape of a thin thread or of a bottle brush, according to the CNTs being oriented parallel or perpendicular to the disclination line, respectively. The system exhibits a rich versatility even if up to now the weak anchorings appear to be difficult to control. As discussed in the associated experimental paper, these necklaces could be a step toward interesting applications for realizing nanowires self-connected in three dimensions to predesignated electrodes. This method could provide a way to increase the number of transistors that may be connected together on a small volume.

DOI: 10.1103/PhysRevE.93.042702

I. INTRODUCTION

In an outstanding work, Poulin *et al.* evidenced a new interaction between water droplets dispersed in a nematic liquid crystal (LC) [1]. The interaction essentially arises from the distortion of the nematic director that the anchoring at the water-LC interface produces in the nematic bulk around the droplets [2]. Though quite simple, the system has, generally, the advantage to exhibit a good reproducibility, the droplets being highly monodisperse with well-defined anchoring conditions. The anchoring is consequently uniform on the droplets, so that they bear a $+1$ topological charge each, which implies a -1 point defect in their vicinity to preserve the zero charge of the whole system [3]. The observation easily extends to systems of isotropic liquid droplets suspended in a nematic LC, as silicone oil droplets [4], or glycerol droplets [5]. Interestingly, these systems allow one to build one-dimensional (1D) and even two-dimensional (2D) sets of spherical droplets that are stabilized by the intercalation of point defects in between them. Similar experiments have also been performed with silica microspheres [6]. They again led to the observation of 1D [7], and 2D [8] sets assembled by means of topological defects. The nematic interaction of particles was further extended to more complex fields than merely uniform. The interaction of particles with disclination lines was thus considered [9]. Surprisingly, the interaction is not radial around a disclination line, so that the trajectory of a particle that is attracted toward a disclination line is not rectilinear. After a while, the particle gets trapped on the disclination. The process is indeed iterative, and more and more particles may get trapped too on the line, and we actually end up with a necklace of micro- or nanoparticles [10]. The disclination line being prepared in order to join opposite electrodes, an electropolymerization technique may be used then to glue the beads to their neighbors. The wire thus automatically goes from one electrode to the associated one, and it conducts enough electricity to allow the synthesis of some polymer between the particles. Finally, the disclination line that worked as a template for guiding the synthesis of the wire may finally be removed. This can be simply achieved on heating the liquid crystal up to the isotropic phase [11]. The wire that is realized in this manner takes the very place of the initial disclination line, and somehow materializes it. Interestingly, the process may be extended to the simultaneous synthesis of a lot of microwires in the three-dimensional space, each one joining predesignated electrodes. Applications for such a possibility could be developed in the near future, allowing a rapid growth of the number of transistors that may be connected together on a small volume. In this manner, Moore's law could be continued even if the downsizing of the circuits that is at its origin comes now to limitations that belong to mesoscopic physics, as tunneling conduction through insulators, or conversely, Coulomb blockade effects that may prevent conduction at nanometric sizes [12].

Symmetry reasons clearly indicate that spherical particles are not well adapted for building 1D wires. Elongated particles, such as, e.g., carbon nanotubes (CNTs), should be more convenient. Moreover, these particles are known for their strength and toughness [13]. They are particularly interesting for producing wires because they generally conduct electricity, and also because they may exhibit extremely large aspect ratios. They should therefore provide the appropriate pieces for building thinner wires, that would offer a reduced drag in the LC, and being more resistant, they should better resist residual flows. Fortunately, experiments show that the CNTs may be dispersed rather well in nematic LCs [14,15],

*yves.galerne@ipcms.unistra.fr

 ©2016 American Physical Society

leading to paranematic phases [16,17]. The use of a surfactant that spreads over the CNT surface may, moreover, help the dispersion of the CNTs in the nematic phase. The surfactant, according to its nature and quantity, changes the wetting properties of the CNTs and may thus favor their dispersion in the nematic bulk. More subtle effects may arise too, as for instance, differential wetting properties with respect to both parts of the liquid crystal molecules, which at the molecular scale arise from the contrast between the London interactions that the CNTs exert on the aromatic and the alkyl parts of the liquid crystal molecule. The surfactant thus governs the differential, i.e., anisotropic, wetting properties of the nematic on the CNT surface, and consequently defines the LC anchoring on the CNTs [18].

As we theoretically show in this paper, the anchoring properties on the CNT surface determine the interaction of the CNT with the nematic director $\boldsymbol{n}$, and consequently they determine its orientation at equilibrium in the $\boldsymbol{n}$ field. In Sec. II, are discussed the cases of the planar, homeotropic, and Janus anchorings, the Janus anchoring being characterized with homeotropic and planar conditions on the opposite sides of each CNT. We consider the strong and weak anchoring cases, where the direction of $\boldsymbol{n}$ is fixed at the CNT surface and where conversely the direction of $\boldsymbol{n}$ is free, respectively. In this latter case, $\boldsymbol{n}$ adjusts at the CNT surface in order not to change the initial distortion, nor consequently, the elastic energy of the $\boldsymbol{n}$ field. The discussion is based on an estimate of the free energy of the whole system that includes the anchoring energy and the elastic energy variations due to the introduction of a CNT in the nematic bulk. Rough estimates are indeed sufficient to conclude in almost each situation. In Sec. III, we similarly discuss the interaction of a CNT with a splay-bend disclination line, and more precisely, we analyze the best way, orientation, and position, that the CNT will adopt when settling on it. The three cases of the planar, homeotropic, and Janus anchorings are again considered. Finally, we conclude in Sec. IV on discussing the respective advantages of the CNTs, and their best anchoring treatments, for realizing nanowires that automatically connect in the three-dimensional (3D) space to predesigned electrodes. In the following paper [19], experimental observations are reported to provide a basis for comparison with these theoretical results, and to complete the discussion on the interactions of CNTs with the director field $\boldsymbol{n}$ and with the disclination lines of the nematic LC that is presented here.

II. CNT ORIENTATION IN A NEMATIC LC

The CNTs, when dispersed in the nematic LC phase, interact with the LC molecules and they finally choose their preferred orientation referred to the direction of the nematic director $\boldsymbol{n}$. In this paper, we study three different anchoring conditions of the LC molecules onto the CNTs—planar, homeotropic, and Janus anchorings (namely, half planar and half homeotropic)—and we examine the manner that the CNTs spontaneously orient in a nematic LC.

A. Planar anchoring

Density functional calculations show that the binding energy of a LC molecule onto a CNT wall is about 2 eV essentially due to London interactions between corresponding benzene rings. This energy is much larger than $kT \sim \frac{1}{40}$ eV, T being the room temperature [20]. This indicates that nude CNTs may be directly dispersed in LCs, and secondly, that the LC molecules prefer to stick tangentially to the CNTs, which corresponds to planar anchoring. We may, moreover, anticipate that the London interaction of multiwall CNTs with the benzene ring body of the LC molecules should be larger than the interaction of single-wall CNTs, because they naturally contain a larger density of benzene rings. They should therefore exhibit stronger planar anchoring properties too.

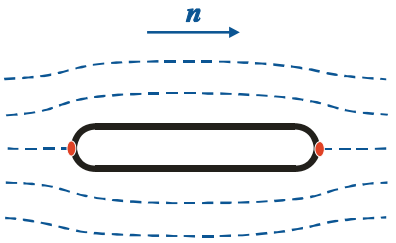

FIG. 1. Schematic representation of the $\boldsymbol{n}$ distortion around a CNT aligned parallel to the director $\boldsymbol{n}$ in a uniformly oriented nematic LC. The oval red dots depict the two boojums on each pole of the CNT.

Among all the possible orientations that satisfy the condition of the nematic director being parallel to the CNT surface, the one that distorts the director field as little as possible and, therefore, that minimizes the elastic energy cost, is clearly realized when both the CNT and the director $\boldsymbol{n}$ are parallel to each other, irrespective of the strong or weak anchoring strength on the CNT. We also notice that a uniform planar anchoring on the CNT implies that it is equivalent to a $+1$ topological defect. Therefore, when the CNT is introduced in a uniformly oriented nematic LC (i.e., of null topological index), companion defects of total indices -1 are necessary in the vicinity of the particle to conserve the sum of the topological indices. Reminiscent to the case of spherical particles dispersed in a nematic phase, two surface point defects of strength $-\frac{1}{2}$, known as boojums [21], then appear on both ends of the CNT (Fig. 1).

As the large CNTs may be observed under a polarizing microscope, we easily verify that the bare CNTs orient parallel to the director as is consistent with the above discussion (Sec. IV A). This feature is particularly striking in the vicinity of a disclination line perpendicular to the sample. Then the CNTs orient parallel to the director as compasses follow the magnetic field in the vicinity of magnets [10,11].

B. Homeotropic anchoring

In order that the CNTs anchor homeotropically the nematic director $\boldsymbol{n}$ on their surface, they have to be covered with chemical orbitals that resemble the tips of liquid crystal molecules [22]. Namely, they have to be coated with aliphatic chains. The LC molecules will then prefer to stand everywhere perpendicularly to the CNT surface. As in the planar case, the particle is topologically equivalent to a $+1$ point defect, which means that, when the CNT is immersed in a uniformly oriented sample, a companion defect of strength -1 must be created

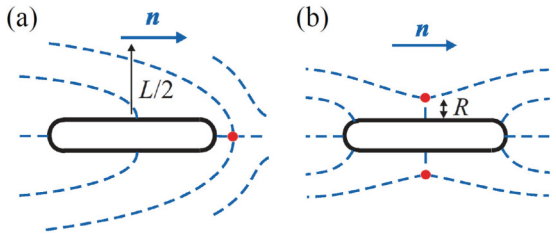

FIG. 2. Cross sections of a CNT with homeotropic anchoring conditions, and oriented parallel to $\boldsymbol{n}$. The whole director field is symmetric around the horizontal axis. Being topologically equivalent to a $+1$ defect, the CNT is accompanied (a) with a -1 point defect at a distance R from the tip, (b) that may open up into a Saturn ring of $-\frac{1}{2}$ disclination line shown as red dots in the cross section, and represented close to the CNT center, this symmetric configuration being probably the stable one.

in the vicinity in order to conserve the total topological index equal to zero [1].

Before beginning calculations, we may make a few general remarks. For the sake of reproducibility, the CNTs of identical anchoring treatments orient preferentially at the same, definite, angle from the nematic director $\boldsymbol{n}$. We may also anticipate that symmetric configurations are characterized by extreme coupling energies. More precisely, the symmetry should not only concern the CNT orientation referred to the general orientation of $\boldsymbol{n}$, namely, the parallel or perpendicular directions. It should also include the whole director field around the CNT. Generally, but this is not an absolute law, the energy varies monotonously as a function of the CNT rotation angle from one of the symmetric orientations to the next one. Then, one of the symmetric orientations corresponds to the lowest energy, and determines the stable orientation. In this case, the preferred CNT orientation is parallel (Fig. 2) or perpendicular (Fig. 3) to $\boldsymbol{n}$. Let us first examine the parallel case. The coupling energy between the CNT and the LC molecules may be calculated from the addition of the elastic energy of the distortion that is produced around the CNT, and of the anchoring energy of the LC molecules on the CNT surface. In order to simplify the evaluation of the elastic energies, we

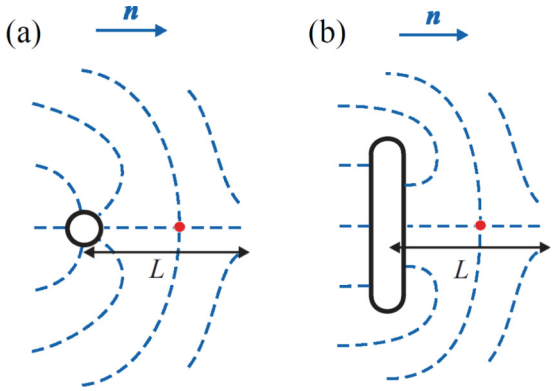

FIG. 3. Director field around a CNT with homeotropic anchoring conditions, introduced in the nematic perpendicularly to $\boldsymbol{n}$. (a) Cross section perpendicular to the CNT, and (b) in the plane of both the CNT axis and of $\boldsymbol{n}$.

suppose the Frank elastic constants to be equal. The $\boldsymbol{n}$ field then satisfies the Laplace equation $\Delta \boldsymbol{n} = 0$, under the constraint $\boldsymbol{n}^2 = 1$. In general, the problem is difficult to solve and needs numerical calculations. However, if we restrict our interest to places far enough from the CNT so the director $\boldsymbol{n}$ is only slightly deviated from its general direction z, the perpendicular components of $\boldsymbol{n}$ are small, and they independently obey the scalar Laplace equation, i.e., they are harmonic functions. As, moreover, we focus on the $\boldsymbol{n}$ solutions that exhibit cylindrical symmetry, the use of cylindrical coordinates is recommended. Then, the perpendicular components of $\boldsymbol{n}$ just reduce to the radial component n_r, which, satisfying the Laplace equation at large distances, is equivalent to an electric potential. For solving the problem, we may thus simply use an electrostatic analogy [2,11]. In the case of infinitely long CNTs, for instance, this allows us to deduce that the distortion extends over an infinite distance perpendicularly to the CNT axis. However, real CNTs have a finite length L. The Laplace equation then shows that the second derivatives in z (along the CNT axis) and in r (along a radial axis) should be on the same order of magnitude [23]. The distortion starting from the CNT center should therefore extend over about the same distance $L/2$ radially as along the CNT axis. This remark is consistent with L being the only relevant distance of the problem. The volume of the distortion is therefore roughly cylindrical, $\sim \frac{\pi}{4} L^3$.

We may now estimate the interaction energy of a CNT colloid with strong homeotropic anchoring when immersed in a uniform $\boldsymbol{n}$ field. The anchoring being strong, the director $\boldsymbol{n}$ is forced to be perpendicular everywhere onto the CNT surface. This implies a distortion around the CNT colloid, and therefore an elastic energy. Conversely, as the director $\boldsymbol{n}$ over the whole CNT surface is along the preferred direction, the anchoring energy is null. The interaction energy of the CNT with the nematic LC then reduces to the elastic energy of the distortion. In the case where the CNT is oriented parallel to $\boldsymbol{n}$ (Fig. 2), we may thus estimate its interaction energy to be

$$W_{\mathrm{str}-h}^{\mathrm{para}} \sim \frac{1}{2} K \left(\frac{\pi}{L}\right)^2 \frac{\pi}{4} L^3 \sim \left(\frac{\pi}{2}\right)^3 KL. \qquad (1)$$

In this expression, we have neglected the energy of the distortion around the CNT tips, because they only extend over a distance equivalent to the CNT radius R, and that R is much smaller than L. We have also evaluated the modulus of the distortion to be $\nabla\theta \sim \frac{\pi}{L}$, since the whole distortion roughly corresponds to a $\pi/2$ rotation over a distance $L/2$. Let us recall that point defects do not produce any singularity in the elastic energy expression contrarily to the equivalent one-dimension defects, namely the disclination lines [2]. Their energy, moreover, stays small here so that we may neglect it. Clearly, this evaluation is rather crude, but it leads to $W_{\mathrm{str}-h}^{\mathrm{para}} \sim 3.87KL$, which is pretty close to the more detailed calculation proposed in the Appendix which yields $W_{\mathrm{str}-h}^{\mathrm{para}} \sim 3.66KL$ [Eq. (A9)].

In the case of thin CNTs, the point defects may evolve towards $-\frac{1}{2}$ disclination loops of radius $2R$ as observed on spherical particles of small radius. The reason for these Saturn rings is that the line tension of disclinations is on the order of K, and that their energy, $4\pi KR$, becomes smaller than the energy of a point defect for $R < 0.2\ \mu$m [3]. When the point

defect changes into a Saturn ring, the director field does not significantly change except in a volume between the CNT and the ring, on the order of $\frac{4\pi}{3}R^3$. With R much smaller than L, the corresponding distortion energy may be neglected in the expression of the coupling energy [Eq. (1)]. We may also wonder if the ring further slides towards the CNT center and stabilizes into the symmetry plane perpendicular to the CNT axis [Fig. 2(b)]. The configuration is then formally equivalent to 2 CNTs of $L/2$ length in head to tail position. As Eq. (1) or (A9) shows, this configuration exhibits a coupling energy on the same order of magnitude as the previous one with the ring around the CNT tip. However, the distortion in the vicinity of the disclination loop should be softer [Fig. 2(b)] than around the hyperbolic point defect [Fig. 2(a)]. We may thus anticipate that the configuration with the Saturn ring being located symmetrically in the CNT center has a lower, and indeed minimum, energy cost. However, this minimum of energy should be confirmed by a specific numerical calculation.

We may similarly estimate the elastic energy of the distortion produced by a CNT with strong homeotropic anchoring, and immersed in the nematic LC perpendicularly to $\boldsymbol{n}$. We obtain

$$W_{\mathrm{str}-h}^{\mathrm{perp}} \sim \frac{1}{2}K\left(\frac{\pi}{L}\right)^2\frac{\pi}{4}L^3 \times 2 \sim 2\left(\frac{\pi}{2}\right)^3 KL. \qquad (2)$$

The distortion extends over a distance about L in the three directions of space as in the previous case of a CNT parallel to $\boldsymbol{n}$. More precisely, the distortion is confined inside a cylinder of radius $L/2$ and length L, centered approximately on the topological point defect, at about a distance $L/2$ from the CNT. Its volume is therefore $\sim\frac{\pi}{4}L^3$. As in the previous case, the distortion roughly makes a $\pi/2$ rotation. However, close to the CNT the distortion increases up to make a π turn and, moreover, it occurs in both planes of Figs. 3(a) and 3(b). This double rotation explains the factor 2 in Eq. (2). We thus obtain $W_{\mathrm{str}-h}^{\mathrm{perp}} \sim 7.74KL$. A more careful estimation is proposed in the Appendix that yields $W_{\mathrm{str}-h}^{\mathrm{perp}} \sim 8.06KL$ [Eq. (A11)], which indeed is rather close. Clearly, to obtain a really better evaluation, numerical models should be used. They would allow one to calculate the real advantage of the parallel orientation over the perpendicular one, in the strong anchoring limit. Nevertheless, in view of the estimates proposed here, we may conclude that $W_{h-\mathrm{el}}^{\mathrm{para}} < W_{h-\mathrm{el}}^{\mathrm{perp}}$ by about a factor of 2. Both configurations being symmetric, the above remark on the minimum coupling energy applies. We may therefore conclude that the preferred orientation of the CNTs under strong homeotropic conditions is indeed parallel to $\boldsymbol{n}$.

Naturally, the anchoring strength is never infinitely strong. For comparison, we may consider the opposite assumption, where the anchoring is weak (but not infinitely weak). Then, there is no extra distortion in the vicinity of the CNT and also no need for any point defect. The coupling energy between the CNT and the $\boldsymbol{n}$ field is just relevant to the anchoring energy, that is nothing else than the anisotropic part of the CNT surface energy in its LC environment. This energy arises from the different orientations between the nematic director $\boldsymbol{n}$ and the easy axis $\boldsymbol{n}_0$ on the CNT surface. To the lowest order, the anchoring energy per surface unit may be defined as an always positive or null quantity by the equation $W_{\mathrm{anch}} = \frac{1}{2}A[1-(\boldsymbol{n_s}\cdot\boldsymbol{n}_0)^2]$, where $\boldsymbol{n_s}$ is the director on the CNT surface, and the anchoring coefficient A is an energy per surface unit [2,24]. The coefficient A may therefore be understood as an energy per unit length divided by a length, where both quantities are characteristic of the nematic liquid crystal. Their orders of magnitude are therefore that of the Frank elastic constant K and of the nematic extrapolation length λ, respectively. So, we may estimate $A \sim K/\lambda$ [2]. In general, the extrapolation length identifies with the only available distance in the nematic phase, which is the molecular length, or more exactly in the case of 5CB, the dimer length, l. However, close to the substrates, the role of the solid interface may complicate this simplified argument and change the value of λ by orders of magnitude. For instance, the azimuthal anchoring constant may be measured to be much below this crude evaluation [25]. Nevertheless, such cases seem to be exceptional. In our experiments, CNTs with $R \sim 100$–150 nm are dispersed in a 5CB nematic LC of dimer length $\sim$3 nm; we may evaluate the ratio $\frac{R}{\lambda}$ to be on the order of 30–50 [19]. This allows us to estimate the anchoring energy that is involved when the anchoring conditions on the CNT are weak. The anchoring on the CNT being unable to disturb the director field, and to produce a distortion around the CNT, the elastic energy vanishes, and the interaction energy between the CNT and the nematic LC reduces to the anchoring energy. In the cases where the CNT is oriented parallel or perpendicular to the average direction of $\boldsymbol{n}$, the anchoring energy, or equivalently, the interaction energy between the CNT and the nematic LC may thus be estimated to be, respectively,

$$W_{w-h}^{\mathrm{para}} \sim \pi ARL \sim \pi K\frac{R}{\lambda}L, \qquad (3)$$

and

$$W_{w-h}^{\mathrm{perp}} \sim \frac{1}{2}A\pi RL \sim \frac{\pi}{2}K\frac{R}{\lambda}L. \qquad (4)$$

In the last expression, we have taken into account that $\boldsymbol{n}$ is already about homeotropic on half of the CNT surface, and that therefore this part of the surface does not contribute to the anchoring energy. We may then estimate the ratios $W_{\mathrm{str}-h}^{\mathrm{para}}/W_{w-h}^{\mathrm{para}} \sim \frac{\pi^2}{8}\frac{\lambda}{R}$ and $W_{\mathrm{str}-h}^{\mathrm{perp}}/W_{w-h}^{\mathrm{perp}} \sim \frac{\pi^2}{2}\frac{\lambda}{R}$. They indicate that except for large extrapolation lengths and small CNT radii, the elastic energies are much larger than the anchoring ones, and that therefore we are generally in the case of infinitely strong anchorings. Then, a simple comparison between Eqs. (1) and (2) shows that the minimum energy is obtained when the CNTs with homeotropic conditions are oriented parallel to the average direction of $\boldsymbol{n}$. In the case of large extrapolation lengths and small CNT radii, conversely, the anchoring is weak and the distortion vanishes. The preferred orientation of the CNTs is then given on comparing the anchoring energies (3) and (4). They show that the CNTs will now prefer to orient perpendicular to the average direction of $\boldsymbol{n}$, i.e., perpendicular to the direction that they take in the strong anchoring case.

In the general case, the anchoring strength is in an intermediate range. Neither the elastic energy of the distortion around the CNT, nor the anchoring energy, may be neglected. The two elastic energies are in series, and they may be identified on following the distortion of the director $\boldsymbol{n}$ in the

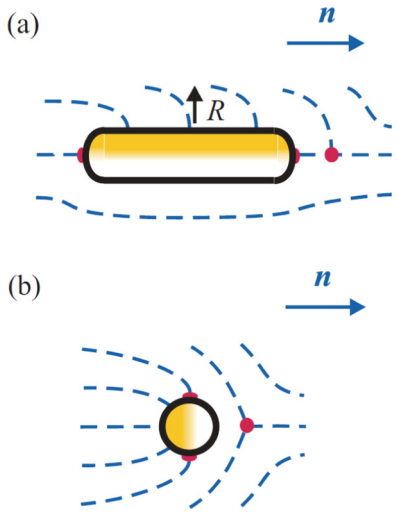

FIG. 4. Cross sections of a Janus CNT and its director field in the case where (a) the CNT axis is parallel to $\boldsymbol{n}$, and (b) perpendicular to $\boldsymbol{n}$. The yellow (white) parts indicate the areas treated for a homeotropic (planar) anchoring, respectively. The oval dots mark surface disclination lines. The circular dot at a distance R from the CNT tip is a $-\frac{1}{2}$ point defect.

nematic cell. Starting from the CNT substrate, we see that the director $\boldsymbol{n}$ first rotates from the easy axis $\boldsymbol{n}_0$ to $\boldsymbol{n}_s$ in the nematic layer in contact with the CNT surface where the anchoring takes place. The director $\boldsymbol{n}$ then continuously rotates along the distortion in the nematic bulk from $\boldsymbol{n}_s$ toward the direction $\boldsymbol{n}_\infty$ away from the CNT particle. The two corresponding energies being of the elastic type, the total energy of the system W obeys a classical theorem, and satisfies the simple equation

$$1/W = 1/W_{\text{anch}} + 1/W_{\text{elast}}, \tag{5}$$

where the distortion energy W_{elast} is obtained under the assumption $\boldsymbol{n}_0 = \boldsymbol{n}_s$, i.e., in the strong anchoring limit, and conversely, the anchoring energy W_{anch} is calculated with the opposite assumption, $\boldsymbol{n}_s = \boldsymbol{n}_\infty$, i.e., in the weak anchoring limit.

C. Janus anchoring

Janus CNTs are prepared [19] in such a way that they exhibit homeotropic and planar anchoring conditions on opposite sides as shown in Figs. 4(a) and 4(b). In this manner, the CNTs may more easily adapt to a complex director field, so that the elastic distortion and the anchoring energies should be significantly reduced if compared to the previous and simpler anchorings. However, these coupling energies are more difficult to estimate.

In the case where the CNTs are oriented parallel to $\boldsymbol{n}$, the elastic and anchoring energies may be evaluated on using the same method as for the full homeotropic case. If the anchoring of the nematic LC on the CNT is strong, we may use again the electric analogy to calculate the distortion field and its elastic energy. The CNT with Janus treatment is equivalent to a dipolar line made of opposite charges spread over two parallel lines at a distance of about R to each other. Therefore, though the distortion in the half space in contact with the homeotropically treated surface appears to be qualitatively the same as in the full homeotropic case [compare Figs. 2(a) and 4(a)], it now extends over a distance of about R only. With a rotation angle of $\frac{\pi}{2}$ over a distance R, and a volume $\sim\frac{\pi}{2}(2R)^2L$, the distortion now has an elastic energy on the order of

$$W_{\text{str}-J}^{\text{para}} \sim 2\left(\frac{\pi}{2}\right)^3 KL, \tag{6}$$

which is twice the elastic energy of the completely homeotropic CNT in the parallel orientation to $\boldsymbol{n}$ [Eq. (1)].

Because of their two types of anchoring, planar and homeotropic, the Janus CNTs bear a $+\frac{1}{2}$ topological defect. This property may be understood rather simply on approaching two Janus CNTs back to back until they come in contact with each other by their planar side. After relaxation, we obtain the distortion field of a completely homeotropic CNT that bears a $+1$ topological index (Sec. II B). We thus deduce that the Janus CNTs should be accompanied by a $-\frac{1}{2}$ point defect when immersed in a uniformly oriented nematic LC. This point defect adds up to the surface disclination line that runs all around the Janus CNT along the border between both surface treatments. This disclination is sketched by two oval red dots in the cross sections of Fig. 4. If the anchoring is infinitely strong, the point defect stays at a distance about R from the tip, but if more realistically the anchoring has an intermediate strength, the point defect migrates toward the CNT tip, and may eventually merge with the surface disclination line for weak enough strengths. In the case of an infinitely weak anchoring, the energy of a Janus CNT in the parallel to $\boldsymbol{n}$ orientation may similarly be estimated to be equal to half the anchoring energy of a homeotropic CNT oriented parallel to $\boldsymbol{n}$ [Eq. (3)]:

$$W_{w-J}^{\text{para}} = \frac{\pi}{2}ARL = \frac{\pi}{2}K\frac{R}{\lambda}L. \tag{7}$$

If a CNT with a strong Janus anchoring is immersed perpendicularly to $\boldsymbol{n}$, the resulting distortion, as noticed above, is equivalent to the one produced by a dipolar line. This shows that the distortion extends over a distance R from the CNT surface and is essentially located in two volumes $\sim R^2L$ each, close to the surface disclination line [Fig. 4(b)]. The associate rotation is less than $\frac{\pi}{2}$ in the average, and partially escapes into the third dimension around the point defect in the planar area, thus reducing the effective curvature of the distortion. Its elastic energy may therefore be estimated to be

$$W_{\text{str}-J}^{\text{perp}} \sim \frac{1}{2}K\left(\frac{1}{R}\right)^2 R^2\, L \times 2 \sim KL, \tag{8}$$

that is about eight times smaller than $W_{\text{str}-J}^{\text{para}}$ [Eq. (6)], which shows that the parallel-to-$\boldsymbol{n}$ orientation of the CNTs is unstable [Fig. 4(a)]. Using again the remark in Sec. II B, we could immediately see that the parallel-to-$\boldsymbol{n}$ orientation cannot be an extremum, because the orientation exhibits only one symmetry element, the plane of Fig. 4(a), that allows dissymmetric and therefore different coupling energies for in-plane CNT oscillations of the same angle. If, conversely, the Janus CNT is oriented perpendicular to $\boldsymbol{n}$, the $\boldsymbol{n}$ field is symmetric about the plane perpendicular to the CNT [Fig. 4(b)]. This ensures that the orientation corresponds to an extremum of the coupling energy between the CNT and $\boldsymbol{n}$. This is clearly a

necessary condition for the coupling energy being a minimum and, so, for the corresponding configuration being stable. So, the CNTs with a strong Janus anchoring preferentially orient perpendicular to $\boldsymbol{n}$. Interestingly, such an orientation is opposite to the stable orientation which was obtained in the completely planar or homeotropic cases.

Conversely, in the weak anchoring case, the integration of the anchoring energy W_{anch} over the CNT surface, except on the caps, is straightforward. This yields

$$W_{w-J}^{\text{perp}} = \frac{\pi}{2} K \frac{R}{\lambda} L, \tag{9}$$

a result that is similar to the case of the Janus CNT in the parallel-to-$\boldsymbol{n}$ orientation [Eq. (7)]. So, in the case of weak anchorings on both Janus CNT sides, the interaction energy between a CNT and the nematic director is rather independent of their relative orientation. In fact, the estimate of the coupling CNT-$\boldsymbol{n}$ energy is too approximate to allow us to deduce the preferred CNT orientation in this case. Numerical calculations are necessary to obtain more precise results.

III. INTERACTION OF A CNT WITH A SPLAY-BEND DISCLINATION LINE

The disclination lines, and in particular, the splay-bend disclination lines, are defects that may be produced at predesigned places in nematic samples provided that the substrates have received appropriate anchoring treatments. Interestingly, the disclinations have been shown to interact with colloids of spherical shape dispersed in a nematic LC [10,11]. As elongated colloids, the CNTs naturally extend this simple case. Because they bear splay and bend multipoles, they couple to the splay and bend components of the distortion field emitted by the disclination lines. From the multipolar interaction energy that results, we may derive the force that drags the CNTs over a long range toward, or away from, the disclination lines. Surprisingly, the force is not radial and consequently, the trajectories of the colloids are not rectilinear [9]. After a while, the CNTs get in contact with the disclination line and they possibly remain trapped on it. A similar phenomenon was evidenced a long time ago in solid crystals where defects are known to condense impurities [26]. To understand the trapping effect, we may estimate the free energy variation of a CNT particle between the two states, far from the disclination line and in contact with it. This needs to estimate the variations of the potential energy and of the entropy between the two states. If the elastic distortion close to the CNT, which depends on the anchoring conditions, resembles the initial distortion around the disclination line, the CNT and the disclination may fit within each other rather well, as a foot in its shoe, without needing an important supplementary energy. (The potential energy contains also an anchoring energy, but for simplicity, we only mention the elastic energy here). A part of the total elastic energy may then be saved in the association. This gain corresponds to the interaction energy between the CNT and the line. For the adhesion of the CNT on the disclination line to be effective, this saved potential energy should be larger than the difference of entropic energies between the two states.

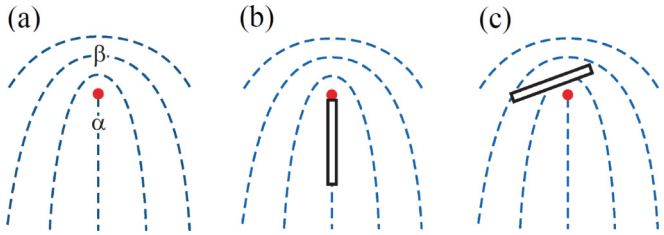

FIG. 5. (a) Pure splay-bend disclination line perpendicular to the figure (red dot). The pure splay (α) and pure bend (β) areas belong to the symmetry plane that contains the disclination line. (b) CNT with planar anchoring, located in the area α, and perpendicular to the disclination. (c) CNT perpendicular to the disclination line, positioned close to the area β, but out of the symmetry plane. The boojums on the CNT tips are not shown.

A. Planar anchoring

As shown in Sec. II A, the CNT colloids with uniform planar anchoring prefer to orient parallel to $\boldsymbol{n}$. This remark *a priori* excludes that the CNTs stabilize parallel or just tilted relative to a splay-bend disclination line after being trapped on it.

They should therefore better stand perpendicular to the disclination, preferentially in a symmetric configuration, that is in the symmetry plane of the splay-bend disclination, in places noted α and β in Fig. 5(a). In both places, the $\boldsymbol{n}$ field is about uniform, so that the distortion field of the disclination is negligibly affected by the presence of a CNT. However, the α and β places are not equivalent. In the splay area α, the CNT stands in the symmetry plane and explores a quasiuniform $\boldsymbol{n}$ field whatever is its length, so that the distortion field of the disclination is negligibly affected by the presence of the CNT [Fig. 5(b)]. The involved extra elastic energy is negligible too, and the planar conditions being satisfied all over the CNT surface, the CNT-disclination interaction energy is minimum, which is consistent with the above remark on the symmetric configurations (Sec. II B) that their coupling energies are extremes. The other symmetric place, the bend area β, where the CNT is perpendicular to the symmetry plane [Fig. 5(c)], is a little less favorable. Due to its length, the CNT is immersed in a less uniform $\boldsymbol{n}$ field so that the match of the anchoring conditions is not so perfect as it was in α. Moreover, the interaction energy is somewhat increased if the CNT, perpendicular to the disclination, is shifted off the symmetry plane. So, the interaction energy between a planar CNT and a disclination, independently of the strong or weak strength of its planar anchoring, is at the minimum in the configuration depicted in Fig. 5(b), and close to it if shifted apart [Fig. 5(c)]. The CNTs with planar anchoring would therefore prefer to stabilize perpendicularly to the disclination line and to lie close to its symmetry plane, independently of their anchoring strength. We may, moreover, notice that if the CNT is in the α place, one of the boojums at its ends may easily coalesce with the core of the disclination line, which could save a supplementary part of the defect energy, adding up to the CNT-disclination interaction energy. However, though the symmetric configuration α corresponds to the lowest energy, it should cost some entropic energy because this configuration is unique [Fig. 5(b)]. So, if the CNTs are somewhat tilted

from the symmetry plane of the disclination, as shown in Fig. 5(c), multiple arrangements become available. Typically, the number of possibilities for setting a planar CNT on a disclination is on the order of the available area in the vicinity of the line, L^2, divided by the projected area of a CNT, LR, that is $\sim L/R$, which leads to a free energy:

$$-T\Delta S \sim -kT\ln(L/R). \tag{10}$$

This entropic energy adds up to the interaction energy of elastic and anchoring natures to determine the free energy that is necessary for condensing a CNT in the symmetry plane of a pure splay-bend disclination line. This term naturally decreases the angular dependence of the CNT free energy interaction with a disclination. We may therefore anticipate that before interacting with one another, i.e., in the absence of direct contact, the CNTs that condense on a disclination line would form a rather disordered structure, in the shape of a bottle brush [Fig. 5(c)]. As more CNTs move toward the disclination line, their density increases on it until they come in contact with one another and stick by means of van der Waals interactions. These interactions being essentially due to London interactions between benzene rings of neighboring CNTs, they are rather strong. The scenario could then evolve a little bit further. The London interaction between close cylindrical objects being proportional to $\sim$–$1/\sin\theta$, where θ is their relative angle [27], the interaction between neighboring CNTs and the torques that they exert on each other, diverge at small θ angles. These torques could be strong enough to force the CNTs to arrange parallel to one another, and therefore to form local ribbons. However, the initial configuration before the CNTs get into contact with one another being *a priori* completely disordered, in the shape of a bottle brush, there are places where the θ angle between neighboring CNTs is large. The aligning torque in these places is then weak and insufficient to overcome the van der Waals adhesion and to orient the CNTs in a common direction. The system should therefore evolve toward local ribbons of different orientations, so that complete ribbonlike structures should be impossible. They would have probably been interesting for applications.

B. Homeotropic anchoring

As spherical colloids, the CNTs with a uniform homeotropic anchoring are topologically equivalent to a $+1$ point defect (Sec. II B). This explains that, when immersed in a nematic LC, they are accompanied by a point defect of -1 topological index located at a distance $d \sim L/2$ (Fig. 3). If the CNT gets trapped onto a disclination line, the point defect may come closer to the CNT than $L/2$ due to the stress exerted by the disclination and because the distortion energy, being proportional to $(\nabla\vec{n})^2 \sim 1/d^2$ multiplied by the distortion volume $\sim d^2L$, does not depend on this distance d to a first order approximation. In a second step, the point defect may open up into a disclination loop of $-\frac{1}{2}$ topological index, provided that its diameter does not exceed a few micrometers [28] [Fig. 2(b)]. However, this limitation may be bypassed if the disclination loop partly merges with the neighboring disclination line. The disclination loop around the CNT may thus elongate, one of its sides merging with the $+\frac{1}{2}$ disclination line and annihilating. Only the other side of the loop, of $-\frac{1}{2}$ topological index, remains and connects to the $+\frac{1}{2}$ disclination line, that consequently just changes sign along the part that runs next to the CNT. The energy cost of the operation is consequently limited to the elimination of the point defect.

Roughly, a CNT with strong homeotropic anchoring, that therefore prefers to point parallel to $\boldsymbol{n}$ (Sec. II B), may get trapped on a splay-bend disclination line essentially along two directions, perpendicular or parallel to the line. In the case that the CNT stands perpendicular to the disclination line, its interaction energy with the disclination corresponds to an extreme if it is located in the symmetry plane or perpendicular to it. Precisely, as in the planar anchoring case (Sec. III A), the interaction energy is minimum when the CNT stands parallel to the symmetry plane in the splay area α [Fig. 5(a)]. The CNT is then oriented parallel to $\boldsymbol{n}$, and the distortion field around it is the same as before its adhesion onto the disclination, so that this configuration does not involve any supplementary elastic energy. The energy gained is therefore restricted to the energy saved by the collapse of the point defect associate to the CNT onto the disclination line. We deduce the interaction energy between the CNT and the disclination to be on the order of

$$E_{\mathrm{str}-h}^{\mathrm{perp}} \sim -W_{\mathrm{core}} \sim -KL, \tag{11}$$

which corresponds to a relatively weak attractive energy [11]. Let us notice that the other symmetric position of the CNT, perpendicular to the symmetry plane in the bend area β [Fig. 5(a)], is less favorable again because this area undergoes a diverging bend close to the core of the disclination line. This naturally implies supplementary elastic and anchoring energies when introducing a straight CNT in it.

The CNTs with strong homeotropic anchoring may also be trapped parallel to the line in the most favorable area α. The energy gain is then given by the addition of the core energy [Eq. (11)] to the elastic energy of the CNT before trapping [Eq. (1)] to which the elastic energy of the distortion contained in the cylinder between the CNT and the disclination line is subtracted [crosshatched area in Fig. 6(a)]. This supplementary distortion is necessary to reconcile the homeotropic orientation of the director on the CNT with the general perpendicular direction of $\boldsymbol{n}$ above the disclination line (area β). Being on the order of $\sim\pi/2$ in a cylinder of diameter d and length L, this distortion costs an elastic energy that may be estimated in the same manner as for establishing Eq. (1):

$$W_{\mathrm{elast}}^{\mathrm{para}} \sim \frac{1}{2}K\left(\frac{\pi}{2d}\right)^2\frac{\pi}{4}d^2L \sim \frac{\pi^3}{2^5}KL. \tag{12}$$

We thus deduce the interaction energy between a disclination line and a CNT, that is trapped parallel to it, to be

$$E_{\mathrm{str}-h}^{\mathrm{para}} \sim -\left\{1+\left(\frac{\pi}{2}\right)^3-\frac{\pi^3}{2^5}\right\}KL \sim -3.9KL, \tag{13}$$

which shows that the CNTs with strong homeotropic anchoring should stay strongly fixed onto the disclination lines, and $E_{\mathrm{str}-h}^{\mathrm{para}}$ being larger than $E_{\mathrm{str}-h}^{\mathrm{perp}}$ (in absolute values), that the CNTs will prefer to orient parallel to the disclination lines in the area α [Fig. 6(a)].

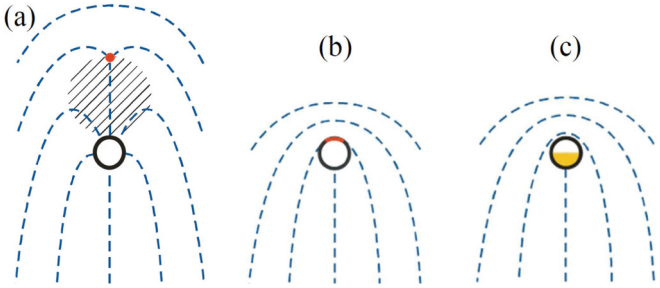

FIG. 6. CNT in interaction with a pure splay-bend disclination line perpendicular to the figure. (a) Case of a strong homeotropic anchoring. The CNT (black open circle) is located at a distance $d < L/2$ in the domain α below the disclination line (red dot). The supplementary distortion that is added to the initial distortion of the disclination when introducing a CNT is roughly contained inside the hatched cylinder of diameter d and length L. (b) Case of a weak homeotropic anchoring. The anchoring breaks on the surface of the CNT are marked in red (gray). This allows the disclination line to vanish inside the CNT. (c) Case of a Janus anchoring. The disclination line vanishes inside the CNT as in (b), but without breaking the anchoring. The lateral disclination lines along the CNT surface are not shown.

Conversely to these CNTs, the CNTs with weak homeotropic anchoring conditions orient perpendicular to $\boldsymbol{n}$ (Sec. II B). If, moreover, they are perpendicular to the disclination line, extremes of the coupling energy are obtained if they are located in the symmetry plane of the splay-bend disclination line. They may then be perpendicular to the symmetry plane in the splay area α, or parallel to it in the bend place β. In this latter case, the $\boldsymbol{n}$ field is quasiuniform around the CNT, so that the anchoring has to break on about half the CNT surface. The interaction energy with the $\boldsymbol{n}$ field is then given by Eq. (4) (Sec. II B):

$$W_{\text{anch}}^{\text{perp}} \sim \frac{\pi}{2} ARL \sim \frac{\pi}{2} K \frac{R}{\lambda} L. \tag{14}$$

After subtraction of the CNT energy before trapping, we obtain the interaction energy of a weakly homeotropic CNT, with a disclination and perpendicular to it, to be

$$E_{w-h}^{\text{perp}} \sim 0. \tag{15}$$

This estimate indicates a rather unfavorable coupling. In the former case (area α), the $\boldsymbol{n}$ field around the CNT is less uniform. The anchoring has to break on a larger area, and the interaction energy with the $\boldsymbol{n}$ field is larger than evaluated above [Eq. (14)]. On subtracting the self-energy of the same CNT immersed perpendicularly to $\boldsymbol{n}$ [Eq. (4)], we obtain a larger interaction energy than in the previous case [Eq. (15)], i.e., a positive energy that shows that the CNT cannot be attracted by the disclination line.

The CNT with weak homeotropic anchoring may also be trapped parallel to the disclination line in the splay area α, the bend area β being clearly less favorable. The anchoring has now to break on less than half the CNT surface [marked in red in Fig. 6(b)] in order to avoid additional distortions around it. The interaction energy with the $\boldsymbol{n}$ field if such a weakly homeotropic CNT is trapped onto the disclination is therefore below the one evaluated for the perpendicular case [Eq. (14)]. After subtracting the self-energy of a CNT immersed in a uniform nematic, we thus evaluate the interaction energy to be negative, which shows that the CNTs with weak homeotropic anchoring get trapped onto disclinations parallel to them in the region α.

Clearly, numerical calculations are necessary to obtain more precise evaluations. They could allow one to know how strongly the CNTs with weak homeotropic anchoring get trapped on the disclination lines. However, in the real cases, the anchoring strength is rarely perfectly weak, so that the interaction energy between CNTs and disclinations should indeed be intermediate, according to Eq. (5). We may therefore anticipate that the interaction energy between CNTs and disclinations will be larger than in the purely weak anchoring cases. The interaction should therefore be attractive, but rather weak and insufficiently efficient for building clean self-connected wires. This suggests to us trying other types of anchoring treatments that are able to solve the intrinsic contradiction of the splay-bend disclination lines that prefer a homeotropic orientation on one side and a planar orientation on the other side.

C. Janus anchoring

In order to improve the trapping efficiency of CNTs onto the splay-bend disclination lines, we now consider Janus anchorings where the CNTs are treated for strong, planar, and homeotropic anchorings on both sides, respectively. As discussed in Sec. II C, the Janus CNTs prefer to orient perpendicular to $\boldsymbol{n}$, and for the same reasons as the CNTs with weak homeotropic anchoring, they will prefer to set parallel to the splay-bend disclination line in the domain α, the distortion that they produce [Fig. 4(b)] fitting rather well inside the disclination distortion. The other symmetric positions are indeed less favorable since they involve an extra distortion of $\boldsymbol{n}$ around them. Therefore, neither supplementary distortion nor breaking of the anchoring are necessary if the Janus CNT is set parallel to the line in the domain α [Fig. 6(c)], so that a part of the self-energy is saved. After subtraction of this self-energy [Eq. (8)], we may estimate the interaction energy of a Janus CNT with a disclination to be

$$E_{\text{str}-J}^{\text{para}} \sim -KL. \tag{16}$$

This shows that the line is able to attract the strong-anchoring-treated Janus CNTs. However, the attraction is weaker than with the strong homeotropic CNTs [Eq. (13)]. This somewhat surprising conclusion results from the large elastic energy involved when dispersing strong homeotropic CNTs in a nematic LC, and that the introduction in the natural distortion field of a splay-bend disclination line will significantly reduce.

Similarly, the interaction energy between a Janus CNT with weak anchoring properties and a splay-bend disclination line may be estimated to be

$$E_{w-J}^{\text{para}} \sim -\frac{\pi}{2} K \frac{R}{\lambda} L. \tag{17}$$

This shows that the interaction is attractive again, at least more than in the case of CNTs with weak homeotropic anchoring.

TABLE I. Preferred CNT orientations, referred to $\boldsymbol{n}$ or to a splay-bend disclination line, according to the planar, homeotropic, or Janus; weak or strong; anchoring on the CNTs.

Anchoring / Interaction with	Planar	Homeotropic		Janus	
		Strong	Weak	Strong	Weak
$\boldsymbol{n}$	//	//	$\perp$	$\perp$	?
Disclination line	$\perp$	//	//	//	//

So, in both cases, the Janus CNTs with strong or weak anchorings should settle along the disclination line and orient parallel to it, which is the most favorable orientation for building clean self-connected wires.

IV. PREFERRED CNT ORIENTATIONS

The energies of CNTs immersed in a nematic LC [Eqs. (1)–(9)] or in contact with a splay-bend disclination line, that have been estimated in Eqs. (11)–(16), allow us to deduce the most stable orientations that the CNTs will adopt according to their anchoring properties, planar, homeotropic, or Janus. Only the case of CNTs treated for a weak Janus anchoring does not lead to clear conclusions, as the two configurations, parallel and perpendicular to $\boldsymbol{n}$, give similar estimates for the CNT-$\boldsymbol{n}$ interaction energy. As mentioned in Sec. II C, numerical calculations would be necessary to determine the equilibrium CNT orientation in this case. Noticeably too, the CNTs with uniform homeotropic treatments are found to orient in a different manner referred to $\boldsymbol{n}$ according to the anchoring strength. However, following Ref. [25], even if a substrate has carefully been prepared for exhibiting a weak anchoring, this property is generally observed to fade out after a while. The cause is a small quantity of large impurity molecules initially solved in the nematic LC, that progressively settle on the substrate and harden its anchoring. For this reason, we do not really observe any stable weak anchoring. Probably, the weak anchorings considered here could remain theoretical only. All the cases discussed above are gathered in Table I.

V. CONCLUSIONS

Whereas spherical colloids dispersed in nematic liquid crystals have been studied for a long time, the use of elongated particles as CNTs has received little attention yet. Their strongly anisotropic shape, however, suggests trying to associate them with nematic LCs. They, moreover, offer rich possibilities of interactions with a uniform nematic field or with disclination lines, if one takes the available types of anchoring into account.

On performing simple evaluations of the anchoring and elastic CNT-$\boldsymbol{n}$ interaction energies, we may predict the orientation of the CNTs in nematic LC dispersions. We thus show that the CNTs stabilize parallel to $\boldsymbol{n}$ in the case of CNTs with strong planar or homeotropic anchorings. In the remaining cases, the CNTs conversely stabilize perpendicular to $\boldsymbol{n}$ except in the weakly anchored Janus case that needs dedicated numerical calculations to be clarified (Table I).

We have also considered the interaction of a CNT with a splay-bend disclination line. The elastic part of the interaction energy essentially arises from the overlap of the distortion fields from both objects. The CNTs may consequently be attracted toward the splay-bend disclination line, and ultimately they settle on it. We have then discussed their orientation at equilibrium on estimating the CNT interaction with the splay-bend disclination line, based on the same method as for calculating the interaction of the CNTs with a uniform nematic field. Again, the CNT orientation depends on the anchoring conditions of the nematic director $\boldsymbol{n}$ on the CNT surface. We thus show that though the CNTs with planar anchoring should stabilize perpendicular to the splay-bend disclination lines, they will come parallel to it in the other cases, i.e., for homeotropic, or Janus anchoring conditions of weak or strong strengths (Table I).

These latter cases may indeed lead to interesting practical applications. For instance, they should result in a large number of CNTs to be attracted to and to fix on a disclination line. We could thus obtain thin nanonecklaces that somehow would realize a materialization of the disclination lines. These points are experimentally addressed in the following paper [19]. Surprisingly, they could help in building 3D self-connected wires at a micro- or nanoscale.

APPENDIX

1. Homeotropic CNT parallel to $\boldsymbol{n}$

The $\boldsymbol{n}$ field around a CNT with homeotropic anchoring conditions [Fig. 2(a)] is the superposition of a radial splay-bend distortion located in the symmetry planes ($\boldsymbol{z}$, $\boldsymbol{r}$), and of an orthoradial splay distortion in the plane perpendicular to the z axis. We may calculate this distortion with reasonable approximations. This will be useful for estimating the elastic energy involved by the CNT. In a first step, we periodize the system on adding CNTs every $2L$ distance along the z axis, a point defect being intercalated between each. We may then expend the field of the distortion $n_r(r,z)$ in a Fourier series in z, each term being a solution of the Laplace equation [23]. Due to the homeotropic anchoring, the z function $n_r(r = R, z)$ is approximately a square function, and the amplitude of its harmonics decreases as the reverse of their order. Their elastic energy respectively decreases as the reverse of the order to the square, and therefore becomes rapidly negligible. For simplicity, we may limit the calculations to the fundamental term of the series that is

$$n_r = f(r)\frac{2}{\pi}\cos\left(\frac{\pi z}{L}\right). \tag{A1}$$

We deduce that $f(r)$ is a solution of the differential equation:

$$f'' + \frac{f'}{r} - \left(\frac{\pi}{L}\right)^2 f = 0. \tag{A2}$$

The solution of this equation is known to be the modified Bessel function K_0, which decreases exponentially as a function of the radial distance r from the CNT. Since we are only interested in orders of magnitude, we may simplify Eq. (A2), and drop its second term. We deduce the approximate

solution, valid for $r > \frac{L}{\pi}$:

$$n_r = \frac{2}{\pi}\cos\left(\frac{\pi z}{L}\right)\exp\left(-\frac{\pi r}{L}\right), \tag{A3}$$

with

$$n_z = \pm\sqrt{1-n_r^2}. \tag{A4}$$

We may then estimate the elastic energy of the distortion per CNT on the line. It is essentially composed of three distortions, a splay and a bend distortion that superpose to a distortion around a hyperbolic point defect [Fig. 2(a)]. With the above expressions of n_r and n_z, we deduce the splay term to be

$$\operatorname{div}\boldsymbol{n} = \left(\frac{1}{r}-\frac{\pi}{L}\right)n_r + \frac{\partial n_z}{\partial z}. \tag{A5}$$

On integrating this divergence to the square over a period $2L$, we deduce the splay distortion energy per CNT. The dominant term is given by the square of the first term in Eq. (A5). It may be evaluated to be worth

$$W_{\text{Splay1}} \sim \frac{4}{\pi}KL\left\{\ln\frac{L}{2\pi R}-\frac{3}{4}\right\}. \tag{A6}$$

With an anisotropic ratio $L/R \sim 35$–50 [19], we deduce $W_{\text{Splay1}} \sim 1.6KL$. The cross term between the two terms of Eq. (A5) yields similarly

$$W_{\text{Splay2}} \sim \frac{2^6}{\pi^2 3^3}KL, \tag{A7}$$

that is, $W_{\text{Splay2}} \sim 0.24KL$. The square of the second term of Eq. (A5) has a negligible contribution, so that we may estimate the total splay contribution to be $W_{\text{Splay}} \sim 1.85KL$.

To this splay energy, we also have to add a bend energy that comes from the square of the bend vector. We deduce

$$W_{\text{Bend}} \sim \frac{19}{16\pi}KL, \tag{A8}$$

that is, $W_{\text{Bend}} \sim 0.38KL$. Adding this bend contribution to the splay one, we get the elastic energy for the fundamental mode to be $2.23KL$. In order to take into account the contribution of the higher order modes, we have roughly to multiply this result by $\sum \frac{1}{n^2} = \frac{\pi^2}{6}$. We thus obtain

$$W_{\text{str}-h}^{\text{para}} \sim 3.66KL. \tag{A9}$$

To this energy, we have also to add the elastic energy of the hyperbolic point defect, which may be easily calculated to be $\frac{8\pi}{3}KR$ [29]. In this expression, R stands for the radius of the distorted region, and therefore corresponds to the CNT radius (Sec. II B). Because the aspect ratio of the CNTs is large, this point defect energy may be neglected compared to $W_{\text{str}-h}^{\text{para}}$ [Eq. (A9)].

2. Homeotropic CNT perpendicular to n

The elastic energy involved by a homeotropic CNT oriented perpendicular to $\boldsymbol{n}$ may be evaluated on starting from a hedgehog distortion (Fig. 3). The distortion extends over a distance $\frac{L}{2}$ and the elastic energy is $\sim \frac{4\pi}{3}KL$. In order to obtain the distortion sketched in Figs. 3(a) and 3(b), we have to apply two supplementary bend distortions of $\frac{\pi}{2}$ angle over a distance $\frac{L}{2}$. On considering that this bend distortion roughly extends over a cylindrical volume of axis parallel to $\boldsymbol{n}$, of length and radius equal to $\frac{L}{2}$, we may estimate the complete elastic energy of the distortion around the CNT to be

$$W_{\text{str}-h}^{\text{perp}} \sim \left\{\frac{4\pi}{3}+\left(\frac{\pi}{2}\right)^3\right\}KL, \tag{A10}$$

i.e., numerically,

$$W_{\text{str}-h}^{\text{perp}} \sim 8.06KL. \tag{A11}$$

[1] Ph. Poulin, H. Starkc T. C. Lubensky, and D. A. Weitz, Science **275**, 1770 (1997).

[2] P.- G. de Gennes and J. Prost, *The Physics of Liquid Crystals* (Clarendon Press, Oxford, 1993).

[3] T. C. Lubensky, D. Pettey, N. Currier, and H. Stark, Phys. Rev. E **57**, 610 (1998).

[4] J.-Ch. Loudet, Ph. Barois, and Ph. Poulin, Nature **407**, 611 (2000).

[5] I. I. Smalyukh, S. Chernyshuk, B. I. Lev, A. B. Nych, U. Ognysta, V. G. Nazarenko, and O. D. Lavrentovich, Phys. Rev. Lett. **93**, 117801 (2004).

[6] I. Musevic, M. Skarabot, U. Tkalec, M. Ravnik, and S. Zumer, Science **313**, 954 (2006).

[7] M. Ravnik, M. Skarabot, S. Zumer, U. Tkalec, I. Poberaj, D. Babic, N. Osterman, and I. Musevic, Phys. Rev. Lett. **99**, 247801 (2007).

[8] U. Tkalec, M. Ravnik, S. Copar, S. Zumer, and I. Musevic, Science **333**, 62 (2011).

[9] D. Pires, J.-B. Fleury, and Y. Galerne, Phys. Rev. Lett. **98**, 247801 (2007).

[10] J.-B. Fleury, D. Pires, and Y. Galerne, Phys. Rev. Lett. **103**, 267801 (2009).

[11] H. Agha, J.-B. Fleury, and Y. Galerne, Eur. Phys. J. E **35**, 82 (2012).

[12] http://en.wikipedia.org/wiki/Moore's law; for more details, see, e.g., H. Iwai, Microelectron. Eng. **86**, 1520 (2009).

[13] E. W. Wong, P. E. Sheehan, and C. M. Lieber, Science **277**, 1971 (1997).

[14] I. Dierking, G. Scalia, and P. Morales, J. Appl. Phys. **97**, 044309 (2005).

[15] R. Basu and G. S. Iannacchione, Appl. Phys. Lett. **93**, 183105 (2008).

[16] P. van der Schoot, V. Popa-Nita, and S. Kralj, J. Phys. Chem. B **112**, 4512 (2008).
[17] V. Popa-Nita and S. Kralj, J. Chem. Phys. **132**, 024902 (2010).
[18] P. Hubert and Y. Galerne, Appl. Phys. Lett. **71**, 1050 (1997).
[19] H. Agha and Y. Galerne, following paper, Phys. Rev. E **93**, 042703 (2016).
[20] K. A. Park, S. Mi Lee, S. Hee Lee, and Y. Hee Lee, J. Phys. Chem. C **111**, 1620 (2007).
[21] O. D. Lavrentovich, Liq. Cryst. **24**, 117 (1998).
[22] J. N. Israelachvili, *Intermolecular and Surface Forces*, 2nd ed. (Academic, New York, 1991).
[23] In order to evidence the symmetry of the problem, we write the Laplace equation in cylindrical coordinates, $\frac{1}{r}\frac{\partial}{\partial r}(r\frac{\partial n_r}{\partial r}) + \frac{\partial^2 n_r}{\partial z^2} = 0$. The two terms have the dimension of a length to the power -2. They are therefore inversely proportional to the square of the characteristic length over which the distortion extends along the radial axis $\boldsymbol{r}$, and along the CNT axis $\boldsymbol{z}$, respectively. Because the two terms cancel, their absolute values are the same, and consequently their two characteristic lengths along $\boldsymbol{r}$ and $\boldsymbol{z}$, are equal, respectively.
[24] G. Barbero and L. R. Evangelista, *Adorption Phenomena and Anchoring Energy in Nematic Liquid Crystals* (Taylor & Francis, London, 2006).
[25] D. Pires and Y. Galerne, Appl. Phys. Lett. **89**, 144110 (2006).
[26] A. H. Cottrell and B. A. Bilby, Proc. Phys. Soc., London, Sect. A **62**, 49 (1949).
[27] R. F. Rajter, R. Podgornik, V. A. Parsegian, R. H. French, and W. Y. Ching, Phys. Rev. B **76**, 045417 (2007).
[28] H. Stark, Eur. Phys. J. B **10**, 311 (1999).
[29] M. Kleman and O. D. Lavrentovich, Philos. Mag. **86**, 4117 (2006).